Wiley
International Journal of Intelligent Systems
Volume 2024, Article ID 7727469, 13 pages
https://doi.org/10.1155/2024/7727469

WILEY

Research Article

Channel Estimation Algorithm Based on Spatial Direction Acquisition and Dynamic-Window Expansion in Massive MIMO System

Shufeng Li,[1] **Baoxin Su**,[1] **Yiming Liu**,[1] **Junwei Zhang**,[1] **and Minglei You**[2]

[1]*The State Key Laboratory of Media Convergence and Communication, School of Information and Communication Engineering, Communication University of China, Dingfuzhuang East Street, Beijing 100024, China*
[2]*PEMC Electrical and Electronic Engineering, University of Nottingham, Nottingham University Park, Nottingham NG7 2RD, UK*

Correspondence should be addressed to Shufeng Li; lishufeng@cuc.edu.cn

Received 22 April 2024; Revised 20 June 2024; Accepted 5 July 2024

Academic Editor: Weiwei Jiang

Millimeter-wave (mmWave) and massive multiple-input multiple-output (MIMO) technologies are critical in current and future communication research. They play an essential role in meeting the demands for high-capacity, high-speed, and low-latency communication brought about by technological advancements. However, existing mmWave channel estimation schemes rely on idealized common sparse channel support assumptions, and their performance significantly degrades when encountering beam squint scenarios. To address this issue, this paper introduces a dynamic support detection window (DSDW) algorithm. This algorithm dynamically adjusts the position and size of the window based on the received signal strength, thereby better capturing signal strength variations and obtaining a more complete set of signal supports. The DSDW algorithm can better capture and utilize the sparsity of the channel, improving the efficiency and accuracy of the channel state information acquisition. By combining the beam-split pattern (BSP) algorithm with the DSDW algorithm, this paper designs an effective method to address the inherent beam-spreading problem in mmWave scenarios. Simulation results are proposed to demonstrate the effectiveness of the BSP-DSDW algorithm.

1. Introduction

To meet the demands of high-speed and high-quality communication, the current configuration of massive multiple-input multiple-output (MIMO) technology cannot meet the demand [1]. Massive MIMO technology involves deploying dozens or even hundreds of antennas at the base station, serving multiple users across multiple frequency bands. This setup efficiently harnesses spatial spectrum resources, thereby mitigating the impact of interference and noise on system capacity. Compared to traditional MIMO technology, massive MIMO offers substantial improvements in spatial multiplexing and spatial diversity, resulting in enhanced system capacity and reliability [2], and therefore the transmission process in massive communication technology requires increased frequency band resources. Owing to the shorter wavelength of millimeter-wave (mmWave) signals and the subsequent reduction in the spacing between adjacent antennas, it becomes feasible to deploy massive antennas in a small form factor [3, 4]. Consequently, the amalgamation of mmWave and massive MIMO technology can compensate for each other's limitations and significantly enhance the overall system performance.

Channel estimation is an essential component of communication systems, particularly in the context of massive MIMO systems. In such systems, challenges such as multipath effects, noise, and interuser interference pose significant hurdles to achieving accurate channel estimation. Precoding and beamforming techniques heavily rely on precise channel state information (CSI) [5], making the accuracy of channel estimation paramount. Given the distinct characteristics of mmWave massive MIMO, traditional MIMO channel estimation methods are inapplicable, necessitating the development of new approaches. In [6], the compressive sampling matching pursuit (CoSaMP) algorithm is employed to enhance channel estimation accuracy and this is achieved by introducing a feedback backtracking process centered around atom selection and broadening the selection scope. The matching pursuit algorithm leverages the sparsity of the channel as a known condition, which impacts the accuracy of the estimation. A sparsity value that is too small results in underfitting of the iterative estimation, while an excessively large value increases algorithm complexity. In reference [7], a sparse adaptive matching pursuit algorithm is proposed to eliminate the reliance on sparsity as a known condition. This method approximates the original signal by adjusting the step size. Meanwhile, the authors in reference [8] take advantage of the inherent sparsity of the mmWave MIMO channel in the angular domain. It reformulates the channel estimation problem as the reconstruction of a compressible signal from noisy linear measurements. In contrast to previous approaches, this method models angular-domain channel coefficients using Laplacian-distributed random variables. Compared to a Gaussian mixture prior, the Laplacian-based algorithm exhibits improved channel estimation accuracy, achievable rate, and computational efficiency. The authors in reference [9] introduce a tensor-based joint channel parameter estimation and information symbol detection scheme. This approach divides the model into an outer submodel and an inner submodel. The inner submodel extracts physical parameters, including angles of arrival/departure (AoA/AoD), Doppler shifts, and complex path gains, from the estimated compound channel matrix. This significantly reduces feedback overhead and enhances estimation accuracy with lower computational complexity. In summary, channel estimation in mmWave massive MIMO systems is a complex task, and these diverse algorithms address various aspects of this challenge, aiming to improve accuracy and efficiency.

To address the challenge of high hardware power consumption in mmWave massive MIMO systems, mmWave massive MIMO systems based on lens antenna arrays have emerged [10]. These systems achieve channel sparsity through the construction of lens antenna arrays, which serve as a foundation for applying compressed sensing techniques. Several algorithms leverage compressed sensing techniques for channel estimation by establishing angular domain estimates. This approach effectively mitigates power consumption and reduces the computational complexity. However, certain channel estimation algorithms, such as convex optimization and the orthogonal matching pursuit (OMP) algorithm, rely on the common sparsity assumption, particularly in mmWave systems. Nevertheless, these algorithms often neglect the interbeam impact resulting from beam splitting.

Beam-split technology in current wireless communication systems, especially in mmWave and terahertz frequency bands, faces a series of technical challenges. Even minor beam errors can cause beam misalignment, affecting signal reception quality and system performance. At high frequencies, channel estimation and tracking become more challenging. Any small environmental changes, such as user movement or object obstruction, can lead to rapid channel variations, and traditional channel estimation algorithms often fall short in these highly dynamic environments. Therefore, channel estimation methods based on beam detection and training have been introduced. The authors in reference [11] analyzed the channel estimation performance of large-scale MIMO Internet of things system in Rayleigh fading by utilizing the least square (LS) and minimum mean square error estimation methods. The authors in reference [12] suggest a channel estimation accuracy improvement through beam search using layered codebooks tailored for mmWave massive MIMO systems. By leveraging the analytical structure of the underlying codeword within the layered codebook, the optimal beam design is derived. The authors in reference [13] designed a beam-split-aware dictionary composed of beam squint correction steering vectors, which inherently includes the effects of beam squint. The proposed beam-split-aware orthogonal matching pursuit method can automatically generate beam squint-corrected physical channel directions, outperforming existing state-of-the-art techniques. The authors in reference [14] proposed a regularized sensing beam-split-based orthogonal matching pursuit scheme. The cascaded channel estimation is formulated as a sparse parameter recovery problem, and the algorithm is utilized to estimate the channel parameters. This approach significantly improves performance in terms of NMSE.

The common sparsity assumption can introduce errors in the carrier direction offset, subsequently leading to a reduction in the accuracy of the channel estimation algorithm [15]. In the context of wideband channel estimation algorithms, assuming a common support set can constrain the algorithm's performance. To overcome this limitation, certain algorithms compute signal power for different beam directions, effectively mitigating the beam diffusion effect [16, 17]. In this work, we propose an algorithm based on the beam-split pattern (BSP) and dynamic support detection window (DSDW) to analyze the beamspace channel and tackle the beam-spreading challenge in mmWave massive MIMO systems. We adopt the Saleh–Valenzuela model for channel modeling while ensuring signal sparsity through the use of a lens antenna array [18]. Initially, the BSP algorithm is employed to establish index sets for various subcarrier directions, aligning them with their corresponding physical channel directions. Subsequently, we calculate the power associated with each index set based on its indices. We design a dynamic window size algorithm to maximize power and compute the support sets for all signals. Finally, the acquired support set aids in signal recovery through an orthogonal matching tracking approach. We present the estimation outcomes of both the BSP and DSDW algorithms and include results from comparative simulation experiments involving existing algorithms.

The main contributions of this paper are as follows:

(1) A channel estimation algorithm for mmWave massive MIMO systems based on dynamic window power capture is proposed. This algorithm addresses the issue of insufficient channel estimation accuracy caused by the beam expansion effect by dynamically adjusting the signal capture window to maximize signal power.

(2) The channel is built upon an angle-domain channel model, and we employ a lens antenna array to focus the incoming signals in specific directions. This transforms the channel into beamspace for signal recovery, effectively mitigating the impact of the beam-spreading effect.

(3) DSDW is executed for each subcarrier, utilizing signal power as the objective function to maximize signal coverage. This approach effectively captures variations in signal strength, optimizing the window's position and size, and thereby obtaining the complete support set of the signal.

The rest of this paper is organized as follows. Section 2 introduces the channel model of the mmWave massive MIMO system. Section 3 introduces an acquisition algorithm based on the beam-splitting effect. In Section 4, the channel estimation scheme based on physical channel direction acquisition and the DSDW algorithm is discussed in detail. Section 5 discusses the performance of the design scheme through simulation. Finally, we summarize the whole paper in Section 6.

2. Channel Model of the mmWave Massive MIMO System

Massive MIMO systems are a key technology for future communication systems, and accurate channel estimation is crucial for achieving effective multiuser diversity and spatial multiplexing. mmWave channels exhibit high-frequency characteristics and sparsity, whereas traditional channel estimation methods perform poorly. Therefore, new methods are needed to adapt to the characteristics of mmWave communication. In addition, accurate CSI is essential for resource allocation, beamforming, and interference management, thereby enhancing the reliability and efficiency of data transmission. Overall, channel estimation can address practical issues in modern communication systems, improve communication performance, and meet the demands of new technologies and applications, thus driving the continuous advancement of wireless communication technology.

Millimeter-wave channels are divided into two major categories: physical models and analytical models. The foundation of physical models is the electromagnetic characteristics between the signal reception and transmission arrays. This type of model can effectively reflect measurement parameters and demonstrate the spatial correlation and sparsity of MIMO systems, as shown in Figure 1, and is also known as a parameterized model. It is commonly used in channel estimation and precoding design. Due to the limited number of scattering paths in millimeter-wave propagation, most research work adopts geometric channel models to describe them. Therefore, this paper also adopts the widely used Saleh–Valenzuela channel model [19].

Assuming there is an available transmission path, also known as a multipath component, between the transmitter and receiver, the transmitter is equipped with a basic uniform linear array (ULA). The narrowband channel fading model can be represented as

$$\mathbf{H} = \sqrt{\frac{N_T N_R}{L}} \sum_{l=1}^{L} \alpha_l \mathbf{a}_R(\theta_l) \mathbf{a}_T^H(\varphi_l), \tag{1}$$

where N_T and N_R are the numbers of antennas at the receiver and transmitter, respectively; α_l is the complex gain of the l-th path; θ_l and φ_l denote the azimuth angles of arrival and departure, respectively, and lie within $[0, 2\pi]$; and $\mathbf{a}_R$ and $\mathbf{a}_T$ represent the receive and transmit array vectors, respectively, and when the antenna array is linear, they are expressed as

$$\mathbf{a}_R(\theta_l) = \frac{1}{\sqrt{N_R}} \left[1, e^{-j2\pi d \sin(\theta_l)/\lambda}, \cdots, e^{-j2\pi (N_T-1) d \sin(\varphi_l)/\lambda}\right]^T,$$
$$\mathbf{a}_T(\varphi_l) = \frac{1}{\sqrt{N_T}} \left[1, e^{-j2\pi d \sin(\varphi_l)/\lambda}, \cdots, e^{-j2\pi (N_T-1) d \sin(\varphi_l)/\lambda}\right]^T, \tag{2}$$

where d and λ represent the antenna spacing and wavelength, respectively, and T denotes the transpose operator. Through the basis expansion model, the newly introduced sparsity can be better reflected. Thus, equation (1) can be written in a compact form represented as follows:

$$\mathbf{H} = \mathbf{A}_R(\boldsymbol{\theta}) \mathrm{diag}(\alpha) \mathbf{A}_T(\boldsymbol{\varphi}), \tag{3}$$

where $\mathbf{A}_R(\boldsymbol{\theta}) = [\mathrm{a}_R(\theta_1), \cdots, \mathrm{a}_R(\theta_L)]$ and $\mathbf{A}_T(\boldsymbol{\varphi}) = [\mathrm{a}_T(\varphi_1), \cdots, \mathrm{a}_T(\varphi_L)]$ contain the steering vectors of each multipath component and the vector $\alpha = \sqrt{N_T N_R / L}[\alpha_1, \cdots, \alpha_L]^T$ contains the gains of the multipath components.

The angle-domain channel model decomposes the channel into multiple paths with specific angles, quantizing these angles to form a channel matrix. This matrix representation of the channel in the angle domain enhances sparsity and simplifies signal processing. The lens antenna array, which combines lens technology with a traditional antenna array, focuses incoming electromagnetic waves such that signals from different directions converge at different positions on the array. This physical focusing mechanism effectively converts the spatial information of the signal into positional information. By placing antennas at the focal plane of the lens, we can capture signals from various directions distinctly. The digital processing of these signals then reconstructs the angle-domain representation of the channel, converting the channel into beamspace. Beam space representation, achieved through beamforming and channel measurement, further sparsifies and consolidates the channel characteristics, thus constructing a beamspace channel matrix. This transformation significantly enhances the efficiency of channel estimation and processing, optimizing overall communication system performance.

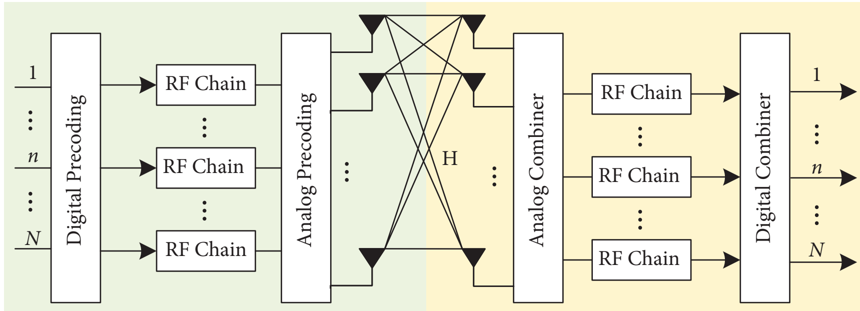

Figure 1: Millimeter-wave massive MIMO system block diagram.

For channel estimation schemes, it is assumed that the presence of a common support set limits the algorithm's performance. Consequently, certain algorithms calculate signal power for different beam directions, thereby effectively addressing the beam-spreading effect. In this section, we construct the system model, which is primarily based on the uplink time-division duplex system under the framework of mmWave massive MIMO. The Saleh–Valenzuela multipath channel model is used, and the antenna array is a ULA [20].

When modeling, the calculation of base stations and users is implemented by an orthogonal frequency guide strategy, which uses Q time slots for sampling. In the uplink training phase, the received signal vector $\mathbf{y}_{l,q} \in N_{RF} \times 1$ on the l-th subcarrier and the q-th time slot can be expressed as

$$\mathbf{y}_{l,q} = \mathbf{A}_q \mathbf{h}_l^b o_{l,q} + \overline{\mathbf{n}}_{l,q}, \quad q = 1, 2, \cdots, Q, \tag{4}$$

where $\mathbf{h}_l^b$ is the broadband channel model, $\mathbf{A}_q$ is the overall combining matrix of $N_{RF} \times N$, $o_{l,q}$ is the transmission pilot on the l-th subcarrier and the q-th time slot, and $\overline{\mathbf{n}}_{l,q} = \mathbf{A}_q \mathbf{n}_{l,q}$, $\mathbf{n}_{l,q} \sim CN(0, \sigma_n^2 \mathbf{I}_N)$ is the Gaussian noise of $N \times 1$. For convenience in analysis, o is set to 1.

The received pilots at the l-th subcarrier are given by

$$\overline{\mathbf{y}}_l = \overline{\mathbf{A}} \mathbf{h}_l^b + \overline{\mathbf{n}}_l, \tag{5}$$

where $\overline{\mathbf{y}}_l = [\overline{\mathbf{y}}_{l,1}^T, \overline{\mathbf{y}}_{l,2}^T, \cdots, \overline{\mathbf{y}}_{l,Q}^T]^T \in C^{N_{RF}Q \times 1}$ and the view matrix is $\overline{\mathbf{A}} = [\overline{\mathbf{A}}_1^T, \overline{\mathbf{A}}_2^T, \cdots, \overline{\mathbf{A}}_Q^T]^T \in C^{N_{RE}Q \times N}$. The multiuser scenario is transformed into a single-user scenario for analysis.

The number of antennas is set to N, the number of users is set to u, and the number of carriers is L. Then, the $N \times 1$ dimensional space channel $\mathbf{h}_l$ of the l-th subcarrier of the user can be written as follows:

$$\mathbf{h}_l = \sqrt{\frac{N}{K}} \sum_{k=1}^{K} \beta_k e^{-j2\pi\tau_k f_l} \mathbf{a}\left(\theta_{k,l}\right), \tag{6}$$

where K, β_k, and τ_k, respectively, represent the number of paths, the complex path gain of the k-th path, and the time delay of the k-th path and f_l is the subcarrier frequency. The space domain array guidance vector $\alpha(\theta_{k,l})$ under the linear antenna array is given by

$$\alpha\left(\theta_{k,l}\right) = \frac{1}{\sqrt{N}} \left[1, e^{-j\pi\theta_{k,l}}, e^{-j2\pi\theta_{k,l}}, \cdots, e^{-j(N-1)\pi\theta_{k,l}}\right]. \tag{7}$$

The $\theta_{k,l}$ can be further expressed as

$$\theta_{k,l} = \frac{2f_l}{c} \mathrm{d} \sin \overline{\varphi}_k, \tag{8}$$

where φ_k is the angle of arrival corresponding to the l-th multipath component, c is the speed of light, $d = c/2f_c$, f_c is the carrier frequency, and f_l is the subcarrier frequency, $f_l = f_c + B/L(l - 1 - (L-1)/2)$. In a broadband system, the center carrier frequency f_c is similar to bandwidth B. The spatial direction of the subcarrier is related to the frequency. Due to the large difference in the spatial direction of each subcarrier in the broadband system, the beam-splitting effect leads to the performance loss of the existing channel estimation schemes.

By converting the spatial channel into the beamspace channel, which is equivalent to performing a matrix transformation, we get

$$\mathbf{P} = \left[\alpha(\overline{\psi}_1), \alpha(\overline{\psi}_2), \cdots, \alpha(\overline{\psi}_N)\right]^H, \tag{9}$$

where $\overline{\psi}_N = 1/N(n - N + 1/2)$, for $n = 1, 2, ..., N$, is the predefined spatial direction of the lens antenna array, as shown in Figure 2. So, the beamspace channel corresponding to the l-th subcarrier $\mathbf{h}_l^b$ can be expressed as

$$\mathbf{h}_l^b = \mathbf{P}\mathbf{h}_l = \sqrt{\frac{N}{K}} \sum_{k=1}^{K} \beta_k e^{-j2\pi\tau_k f_l} \mathbf{b}_{k,l}, \tag{10}$$

where $\mathbf{b}_{k,l} = \mathbf{P}\alpha(\theta_{k,l})$ represents the path component of the beamspace subcarrier, given by

$$\mathbf{b}_{k,l} = \mathbf{P}\alpha\left(\theta_{k,l}\right) = \left[\mu\left(\theta_{k,l} - \overline{\theta}_1\right), \cdots, \mu\left(\theta_{k,l} - \overline{\theta}_N\right)\right]^T. \tag{11}$$

Here, we can observe the characteristics of $\mu(x) = (\sin N\pi x/2)/(\sin \pi x/2)$ from the power concentration of the Dirichlet function. On the other hand, the power of $\mathbf{b}_{k,l}$ is concentrated in the direction of the spatial channel. Since the number of paths is usually small, the sparsity of the angular-domain channel for different subcarriers is primarily determined by $\theta_{k,l}$. This means that in wideband systems, variations in azimuth angles also have a significant impact on signal gain.

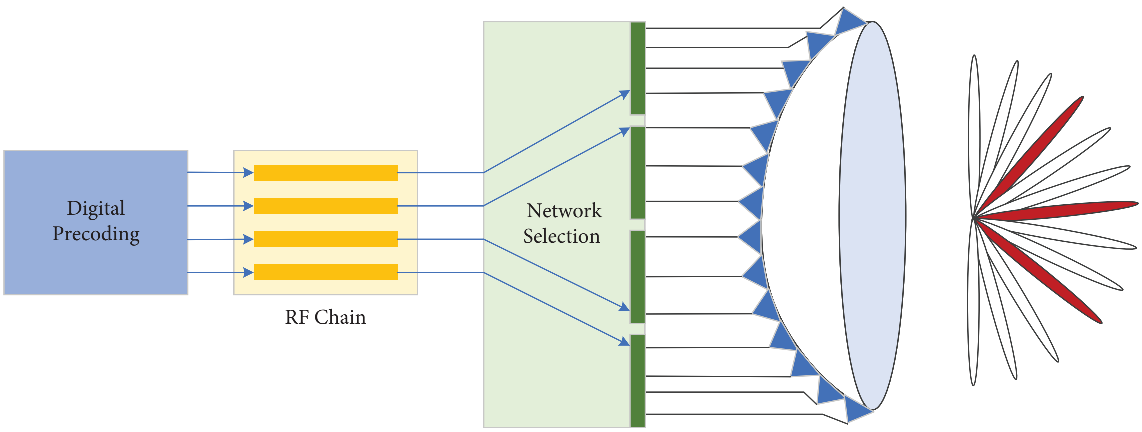

Figure 2: Lens antenna array structure diagram.

3. Acquisition Algorithm Based on Beam-Splitting Effect

As the demand for higher rates and capacity increases, large-scale MIMO systems are predominantly based on wideband systems. This introduces a phenomenon known as beam spread, where the beam direction changes with frequency. Consequently, some algorithms based on the common sparse assumption may introduce errors due to carrier direction offset, leading to a decrease in the accuracy of channel estimation algorithms, particularly those relying on angle-of-arrival-based channel estimation. In this study, we also consider the common sparse assumption in the beamspace in Section 4, jointly addressing the spread effect using the BSP algorithm and the SDW algorithm. In this section, the BSP and SDW algorithms are proposed. For the wave number splitting case, we analyze the relationship between the physical channel direction and the beam direction. After obtaining the beamspace direction [21], we use the SDW algorithm to perform the power maximization calculation and then construct the channel estimation scheme.

3.1. BSP Algorithm for Physical Channel Direction Capture. According to the derivation related to the spatial direction in Section 2, the $\theta_{k,l}$ determines the sparse channel support of the channel $\mathbf{h}_l^b$. In this paper, we consider an algorithm to capture the physical channel direction, referring to the idea of the SOMP algorithm. Let φ_k be the physical channel direction of an arbitrary path, and we define that

$$\mathrm{B}_n = \left[\mathbf{b}_{k,1}, \mathbf{b}_{k,2}, \cdots, \mathbf{b}_{k,l}, \cdots, \mathbf{b}_{k,L}\right]. \tag{12}$$

It is assumed that the physical channel direction φ_k is in the sample $\overline{\theta}_n$ direction of the angle domain, that is, $\varphi_k = \overline{\theta}_n$, and $n_1 \in \{1, 2, \cdots, N\}$. Then, index $\mathbf{b}_{k,l}$ is given by

$$n_{k,l}^{\max} = \arg\min_{n_1} \left|\theta_{k,l} - \overline{\theta}_{n_1}\right| = \arg\min_{n_1} \left|\frac{f_l}{f_c}\overline{\theta}_n - \overline{\theta}_{n_1}\right|, \tag{13}$$

$$\xi_n = \bigcup_{l=1}^{L} \left\{ \left(\arg\min_{n_1} \left|\frac{f_l}{f_c}\overline{\theta}_n - \overline{\theta}_{n_1}\right|, l \right) \right\}, \tag{14}$$

where $\overline{\theta}_n$ is the direction corresponding to the physical channel direction. To prove the effectiveness, we define a physical channel direction $\varphi_{k_0} = \overline{\theta}_{n_0} = \overline{\theta}_n + 2b/N$, where b is a nonzero value, and according to (13), it can be inferred that

$$n_{k_0,l}^{\max} = \arg\min_{n_1} \left|\frac{f_L}{f_c}\left(\overline{\theta}_n + \frac{2b}{N}\right) - \overline{\theta}_{n_1}\right|. \tag{15}$$

According to (13) and (15), we get $|n_{k_0,L}^{\max} - n_{k,L}^{\max}| \geq b$; so, for the specific physical channel direction φ_k, the power captured by the BSP algorithm is

$$\left\|\mathbf{B}_n(\xi_n)\right\|_2^2 = \sum_{l=1}^{L-1} \mu^2\left(\frac{f_l}{f_c}\overline{\theta}_n - n_{k,l}^{\max}\right) + \mu^2\left(\frac{f_L}{f_c}\overline{\theta}_n - n_{k,L}^{\max}\right), \tag{16}$$

$$\left\|\mathbf{B}_n(\xi_n)\right\|_2^2 > \sum_{l=1}^{L-1} \mu^2\left(\frac{f_l}{f_c}\overline{\theta}_n - n_{k,l}^{\max}\right) + \mu^2\left(\frac{f_L}{f_c}\overline{\theta}_n - n_{k_0,L}^{\max}\right) \geq \left\|\mathbf{B}_n\left(\xi_{n_0}\right)\right\|_2^2. \tag{17}$$

Since $\varphi_k = \overline{\theta}_n$, $\mathbf{B}_n(\xi_n)$ can capture more power than $\mathbf{B}_n(\xi_{n_0})$. $\mathbf{B}_n(\xi_n)$ corresponds to the only physical channel direction $\overline{\theta}_n$, and it is also determined by that direction [22].

3.2. SDW Algorithm Based on Window Capture. As depicted in Figure 3, the BSP algorithm proves effective in precisely determining the physical channel's direction, extracting its

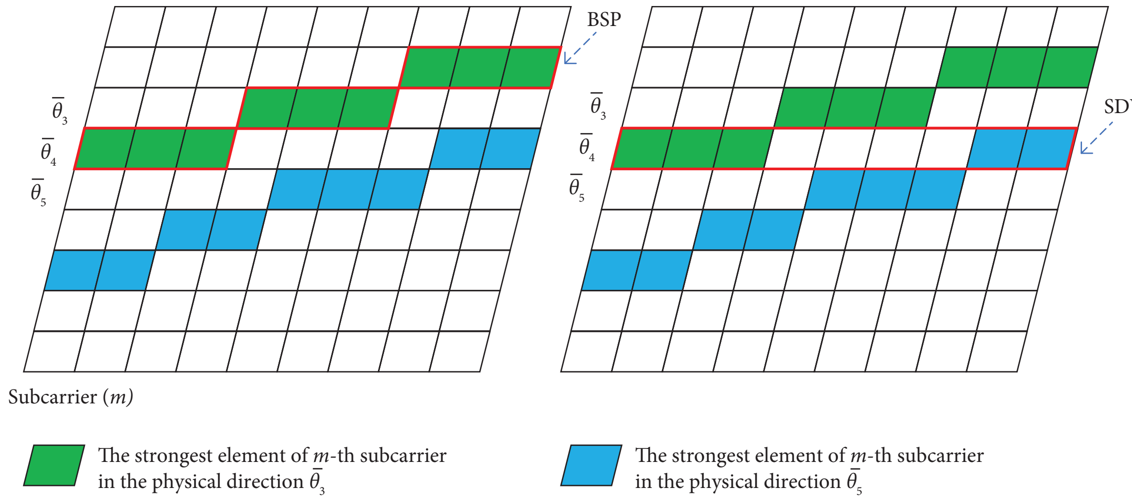

FIGURE 3: Schematic diagram of the physical channel direction capture.

eigenvalues, and consequently capturing its maximum power [23]. In contrast, the common window expansion method, widely used in signal processing, extends a signal segment to analyze more data points but has notable limitations for accurate direction localization. It causes a "smearing" effect, obscuring precise timing information, and introduces phase ambiguities, complicating the interpretation of phase differences crucial for determining signal direction. In addition, it suffers from a resolution trade-off, reducing the time resolution essential for localization, and can integrate more noise, masking subtle differences needed for detecting the signal's origin. To address these issues, alternative techniques such as beamforming, cross-correlation, and adaptive filtering are employed, offering improved accuracy by focusing on specific directions, analyzing time delays, and dynamically adjusting parameters. Due to the wave number splitting effect, subcarriers in other directions also contribute to channel power in a particular direction, leading to estimation errors.

For the support detection window (SDW) algorithm, the window expansion method is realized by expanding the physical channel direction of the BSP algorithm, where λ is the size of the SDW algorithm window and $\sigma_N(x) = \mathrm{mod}_N(x-1)+1$ is the module function, which can be used to ensure that the elements are all nonzero positive integers.

Thus, the ratio of the power captured by the SDW algorithm to the actual power in the direction can be obtained as

$$\gamma = \frac{1}{2N}\sum_{b=-\lambda}^{\lambda}\int_{-1/N}^{1/N}\mu^2\left(\lambda\theta - \frac{2b}{N}\right)\mathrm{d}\lambda\,\theta,$$
$$\gamma = \frac{\sum_{b=-\lambda}^{\lambda}\left\|\mathrm{B}_n\left(\sigma_N\left(\xi_n + b\right)\right)\right\|_F^2}{\left\|\mathrm{B}_n\right\|_F^2}. \tag{18}$$

Due to the power issues involved, $\left\|\mathrm{B}_n\right\|_F^2 = \sum_{l=1}^{L}\left\|\mathbf{b}_{k,l}\right\|_F^2 = MN^2$, combined with the SDW algorithm, we can get

$$\gamma = \frac{1}{MN^2}\sum_{b=-\lambda}^{\lambda}\sum_{l=1}^{L}\mu^2\left(\theta_{k,l} - \bar{\theta}_{n_{k,l}^{\max}+b}\right). \tag{19}$$

As $\bar{\theta}_{n_{k,l}^{\max}+b} = \bar{\theta}_{n_{k,l}^{\max}+b} + 2b/N$ is defined and $\Delta\theta_l = \theta_{k,l} - \bar{\theta}_{n_{k,l}^{\max}}$, then the proportion can be further obtained as

$$\gamma = \frac{1}{LN^2}\sum_{b=-\lambda}^{\lambda}\sum_{l=1}^{L}\mu^2\left(\lambda\theta_l - \frac{2b}{N}\right), \tag{20}$$

where $\Delta\theta_l \in [-1/N, 1/N]$, assuming that they are uniformly distributed, so $\Delta\theta_l = -1/N + (l-1)2/NL$. The sum of all subcarriers is given by

$$\sum_{l=1}^{L}\mu^2\left(\lambda\theta - \frac{2b}{N}\right) = \frac{\mathrm{LN}}{2}\int_{-1/N}^{1/N}\mu^2\left(\lambda\theta - \frac{2b}{N}\right)d\lambda\,\theta. \tag{21}$$

This derivation also verifies the rationality of (16).

4. Channel Estimation Scheme Based on Physical Channel Direction Capture and Dynamic-Window Expansion

This section utilizes BSP and SDW algorithms to develop a DSDW algorithm grounded in physical orientation. Initially, the BSP algorithm is employed to ascertain the index set of distinct subcarriers within the channel model. This approach resolves the issue of beam splitting across various directions and yields the corresponding physical orientations of the index set. Subsequently, the SDW window expansion algorithm is examined to ascertain the accuracy of its capture direction and the size of window expansion by evaluating the power captured by the support set.

4.1. OMP and SOMP Algorithms. The OMP algorithm is a representative of greedy algorithms. Its basic idea is to use iterations for recovery, solving the correlation of the sensing matrix A and the residual matrix to obtain the column with the maximum correlation, and then updating the residual. It gradually updates its atomic support set. The algorithm steps are shown in Algorithm 1.

The SOMP algorithm maintains the sparsity of the solution at each iteration, meaning it only selects atoms most relevant to the residual rather than selecting all atoms relevant to the residual, as in OMP. Therefore, theoretically, SOMP can converge to the optimal solution faster than OMP because it is more sparse. However, SOMP may be computationally more complex as it requires calculating the correlation coefficients between all atoms and the residual. Different from the OMP algorithm, the SOMP algorithm is mainly reflected in the third step of the residual update method. The SOMP algorithm uses a set of joint sparse signals for processing. It can be defined as

$$\mathbf{b}_\lambda = \underset{j=1,2,\ldots,M}{\arg\max} \left| \left\langle \mathbf{r}_j^{t-1}, \mathbf{A}_j \right\rangle \right|. \tag{22}$$

After obtaining the physical channel direction index set, channel estimation can be directly performed based on the SOMP algorithm.

4.2. Research on BSP-DSDW Channel Estimation Scheme. The DSDW algorithm dynamically adjusts the position and size of the window based on the received signal strength. This adaptive mechanism captures signal strength variations more effectively, resulting in a more complete signal support set and further optimized CSI acquisition. By performing signal recovery in beamspace, the DSDW algorithm effectively focuses on the incoming signal in a specific direction, mitigating the negative impact of beam spreading on CSI. Utilizing signal power as the objective function for optimization, the DSDW algorithm better captures and leverages the sparsity of the channel, thereby enhancing the efficiency and accuracy of CSI acquisition. Due to its ability to dynamically adapt to different signal conditions, the DSDW algorithm demonstrates high robustness and reliability in various environments and scenarios, which is crucial for stable communication in practical applications. By improving CSI accuracy, the DSDW algorithm significantly enhances beamforming efficiency, thereby increasing system throughput and reliability, which is of great importance for real-world mmWave massive MIMO systems.

In the previous research study, we established a one-to-one correspondence between the index of the physical channel direction and the physical channel direction itself. This foundational work allowed us to calculate the maximum power of each subcarrier by expanding the window in the physical channel direction, thus obtaining their respective maximum power. Leveraging the insights gained from these algorithms, we can estimate the direction of different subcarriers within the spatial channel. Building upon these principles, we propose a dynamic window acquisition method for broadband channel estimation. This method utilizes the dynamic support detection window (DSDW) for each subcarrier, employing signal power as the objective function. Initially, parameters and weights are set for each subcarrier, followed by signal sampling and analysis. Subsequently, the signal power of each subcarrier is computed as the objective function value. Based on this value, the size and position of the detection window are iteratively adjusted to maximize signal power. Through continuous optimization using algorithms such as gradient descent, the DSDW method selects subcarriers with maximum signal power to form a complete support set, thereby enhancing overall signal coverage.

Step 1: Define a residual matrix $\mathbf{U} \in C^{QN_{RF} \times L}$ and initialize the residual matrix $\mathbf{U} = [\mathbf{u}_1, \mathbf{u}_2, \cdots, \mathbf{u}_L] = \mathbf{Y}$, where $\mathbf{u}_l$ represents the residual of the m-th subcarrier.

Step 2: According to the BSP algorithm based on (14) and (21), set N indexes to estimate N directions to get BSP.

Step 3: Refer to other algorithms to set a correlation matrix. Before that, we write (5) as a matrix and further derive the following equation:

$$\overline{\mathbf{Y}} = \overline{\mathbf{A}\mathbf{H}}^b + \overline{\mathbf{N}}, \tag{23}$$

where $\overline{\mathbf{Y}} = [\overline{\mathbf{y}}_1, \overline{\mathbf{y}}_2, \cdots, \overline{\mathbf{y}}_L]$, $\overline{\mathbf{H}}^b = [\overline{\mathbf{h}}_1^b, \overline{\mathbf{h}}_2^b, \cdots, \overline{\mathbf{h}}_L^b]$, and $\overline{\mathbf{N}} = [\overline{\mathbf{N}}_1, \overline{\mathbf{N}}_2, \cdots, \overline{\mathbf{N}}_L]$. The correlation matrix is constructed as $\mathbf{W} = \overline{\mathbf{A}}^H \mathbf{U}$.

Step 4: The BSP algorithm is used to capture the subcarrier physical channel direction of the correlation matrix $\mathbf{W}$ and obtain the index of different path components as $n_k^* = \operatorname{argmax} \|\mathbf{W}(\xi_n)\|_F$. This step ensures the accuracy of the $\varphi_k = \overline{\theta}_{n_k^*}$ physical channel direction.

Step 5: Use the determined path index to carry out the window expansion algorithm to determine the beamspace sparse channel support of different subcarriers. When the window size is obtained, the dynamic power calculation method is used to determine the window size λ, and the physical channel direction $\overline{\theta}_{n_k^*}$ estimated by the extended BSP algorithm is determined, given by $\gamma_k = \cup_{-\lambda}^{\lambda} \sigma_N(\xi_n + \lambda)$.

Step 6: Eliminate the influence of other paths and calculate the subcarrier channel index $\gamma_{k,l} = \{i \mid (i, m) \in \gamma_k\}$ of each path.

Step 7 and Step 8: According to the obtained support set $\gamma_{k,l}$, the LS method is used to estimate the nonzero element value of the path component and update the residual value. These steps are calculated in each path, and the channel index support sets of all paths are calculated.

Step 9: Merge all the support sets. Finally, the beam channel is estimated by the obtained support set.

The algorithm process is presented in Algorithm 2.

In the process of algorithm development in this paper, we drew references from the OMP algorithm and the SOMP algorithm [24, 25]. The SOMP algorithm is designed for scenarios where sparse signals share the same support set. Unlike the first type of joint sparse model, each group lacks its distinct sparse component. The SOMP algorithm involves calculating inner products and selecting the maximum

Input: measurement matrix $\mathbf{A}$; measurement signal $\mathbf{y}$; sparsity $\mathbf{s}$
Output: channel vector $\tilde{\mathbf{h}}$
(1) Residual signal $\mathbf{r}_0 = \mathbf{y}$ at initialization, atomic support set $\Omega_0 \neq \varnothing$
(2) for $t = 1 : s$
(3) Find the column vector $\mathbf{b}_\lambda$ corresponding to the largest coefficient in the measurement matrix $\mathbf{A}$, record λ_t as the column number, and select the atom $\mathbf{b}_\lambda = \arg \max_{j=1,2,\ldots,M} |\langle \mathbf{r}_{t-1}, \mathbf{A}_j \rangle|$ according to the inner product maximization
(4) Add the obtained sequence number to the atomic support set $\Omega_t = \Omega_{t-1} \cup \{\lambda_t\}$, and then update the matrix $\mathbf{A}_t = \mathbf{A}_{t-1} \cup \{b_{\lambda_t}\}$
(5) Finally estimate the signal $\tilde{\mathbf{h}}_t = (\mathbf{A}_t^T \mathbf{A}_t)^{-1} \mathbf{A}_t^T \mathbf{y}$ through the least squares principle
(6) Update the residual signal $\mathbf{r}_t = \mathbf{y} - \tilde{\mathbf{h}}_t \mathbf{A}_t$.
(7) end for
(8) return $\mathbf{H} = [\tilde{\mathbf{h}}_1, \tilde{\mathbf{h}}_2, \cdots, \tilde{\mathbf{h}}_t]$

Algorithm 1: OMP algorithm.

Input: view matrix $\overline{\mathbf{Y}}$; overall matrix $\overline{\mathbf{A}}$; number of paths K
Output: beamspace channel $\overline{\mathbf{H}}^b = [\overline{\mathbf{h}}_1^b, \overline{\mathbf{h}}_2^b, \cdots, \overline{\mathbf{h}}_L^b]$
(1) Initialize the residual matrix $\mathbf{U} = [\mathbf{u}_1, \mathbf{u}_2, \cdots, \mathbf{u}_L] = \mathbf{Y}$
(2) From (14) get $\xi_n = \cup_{l=1}^{L} \{(\arg\min_{n_1} |f_l / f_c \overline{\theta}_n - \overline{\theta}_{n_1}|, l)\}$
(3) for $k \in \{1, 2, \cdots, K\}$ do
(4) Get the correlation matrix $\mathbf{W} = \overline{\mathbf{A}}^H \mathbf{U}$
(5) Get the index of different path components as $n_k^* = \arg\max \|\mathbf{W}(\xi_n)\|_F$
(6) Estimate physical channel direction $\gamma_k = \cup_{-\lambda}^{\lambda} \sigma_N (\xi_{n_k^*} + \lambda)$
(7) for $l \in \{1, 2, \cdots, L\}$ do
(8) Calculate the subcarrier channel index for each path $\gamma_{k,l} = \{i \mid (i, l) \in \gamma_k\}$
(9) Estimated path component nonzero element values $\mathbf{b}_{k,l}(\gamma_{k,l}) = [(\overline{\mathbf{A}}^H (:, \gamma_{k,l}) \overline{\mathbf{A}} (:, \gamma_{k,l}))]^{-1} \overline{\mathbf{A}}^H (:, \gamma_{k,l}) \mathbf{U}_l$
(10) Update residual value $\mathbf{U}_l = \mathbf{U}_l - \overline{\mathbf{A}} (:, \gamma_{k,l}) \mathbf{b}_{k,l} (\gamma_{k,l})$
(11) Merge support set $\Omega_l = \gamma_{k,l} \cup \gamma_{k-1,l}$
(12) Estimate beam channels $\overline{\mathbf{h}}_l^b (\Omega_l) = [(\overline{\mathbf{A}} (:, \Omega_l) * \overline{\mathbf{A}}^H (:, \Omega_l))]^{-1} \overline{\mathbf{A}}^H (:, \Omega_l) \overline{\mathbf{y}}_l$
(13) end for
(14) end for
(15) return $\overline{\mathbf{H}}^b = [\overline{\mathbf{h}}_1^b, \overline{\mathbf{h}}_2^b, \cdots, \overline{\mathbf{h}}_L^b]$

Algorithm 2: BSP dynamic window expansion capture algorithm.

column number of the computed inner product values as the support set element. It proceeds to obtain the least squares solution and calculate the residual, which then guides subsequent iterations with updates based on the residual. With the assumption of the same support set, column-by-column detection becomes feasible, and each column corresponds to a specific physical channel direction.

In contrast to the SOMP algorithm, the approach presented in this paper divides the iterative estimation process into two steps. Initially, we employ the BSP algorithm to compute the physical channel direction for each subcarrier. This critical step addresses the issue of direction estimation errors induced by wave number splitting in broadband systems. Following the determination of the physical channel direction, the support set expands dynamically based on the estimated physical channel direction. This step establishes the dynamic window size through the acquisition of maximum power. In summary, within broadband systems, we no longer rely on the estimated direction under the ideal assumption for estimation, thereby significantly reducing performance loss due to the resolution of the direction deviation problem caused by the beam-splitting effect. Consequently, accurate subcarrier support sets can be obtained in broadband systems, leading to heightened estimation accuracy.

4.3. Algorithm Complexity Analysis. From Algorithm 2, we can see that the complexity is mainly concentrated in Steps 4, 5, 9, 10, and 15.

The calculation of the correlation matrix is included in the operation of Step 4. As $\overline{\mathbf{A}} \in C^{N_{RF}Q \times N}$, $\mathbf{U} \in C^{QN_{RF} \times L}$, the calculation complexity of Step 4 is $\mathrm{O}(N_{RF}PNL)$.

In Step 5, the norm of $\mathbf{W}(\xi_n)$ is calculated. The size of it is $L \times 1$ and calculated N times, and the calculation complexity is $O(NL)$.

In Step 9, we calculate the nonzero value of each subcarrier, complete the LS calculation of the matrix, and solve the product of the generalized inverse of matrix $\overline{\mathbf{A}}(:, \gamma_{k,l}) \in C^{N_{RF}Q \times (2\lambda+1)}$ and the residual matrix $\mathbf{u}_l \in C^{N_{RF}Q \times 1}$, so the complexity is $\mathrm{O}(LN_{RF}Q\lambda^2)$.

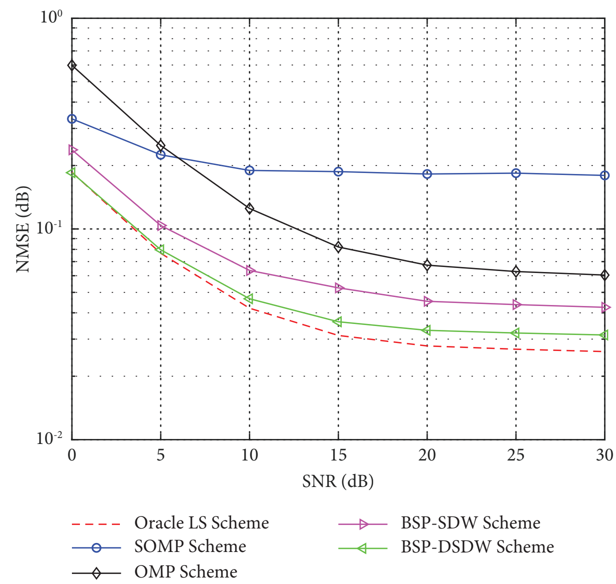

Figure 4: NMSE under different SNRs.

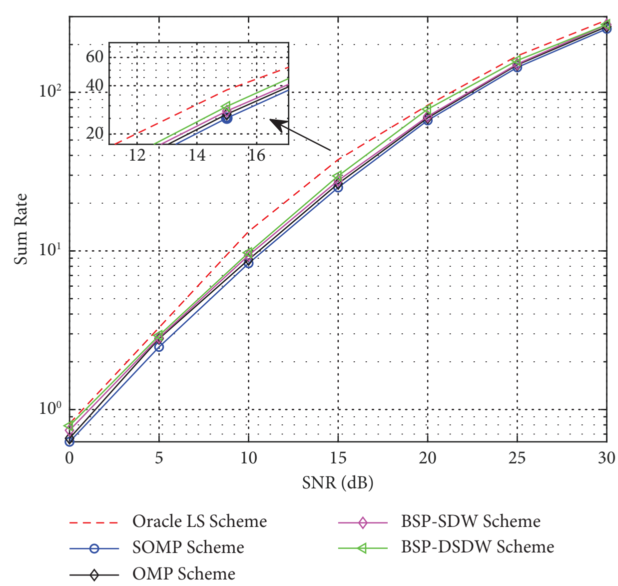

Figure 5: Sum rate under different SNRs.

Similarly, Step 10 involves the calculation of matrix $\mathbf{b}_{k,l}(\gamma_{k,l}) \in C^{N_{RF}Q\times 1}$, with a complexity of $O(LN_{RF}Q\lambda)$.

Step 15 is subcarrier channel restoration, which uses the support set after combining the path components. Compared with Step 9, the cycle calculation of the path components is increased and the complexity is $O(\mathrm{LN_{RF}QK^2}\lambda^2)$.

Finally, we consider the number of paths executed in Steps 4, 5, 9, 10, and 15. The total complexity O is expressed as

$$O = \mathrm{O}(\mathrm{LNN_{RF}QK}) + \mathrm{O}(\mathrm{LNK}) + \mathrm{O}\left(\mathrm{LN_{RF}QK}\lambda^2\right) + \mathrm{O}\left(\mathrm{LN_{RF}}QK^2\lambda^2\right). \tag{24}$$

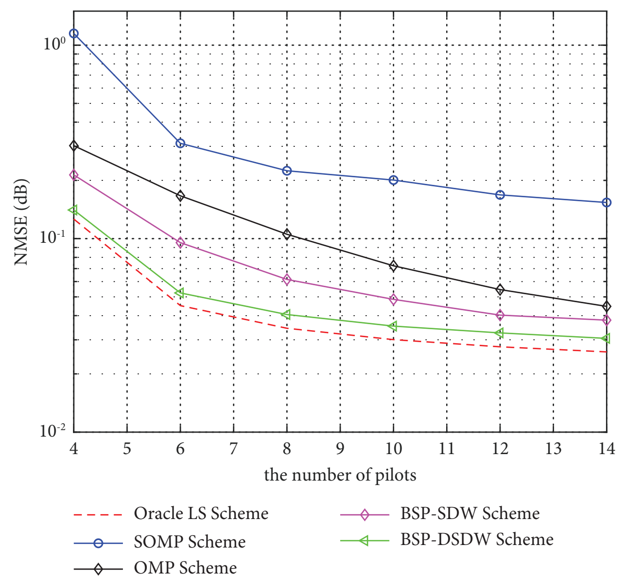

Figure 6: NMSE of pilot length algorithms.

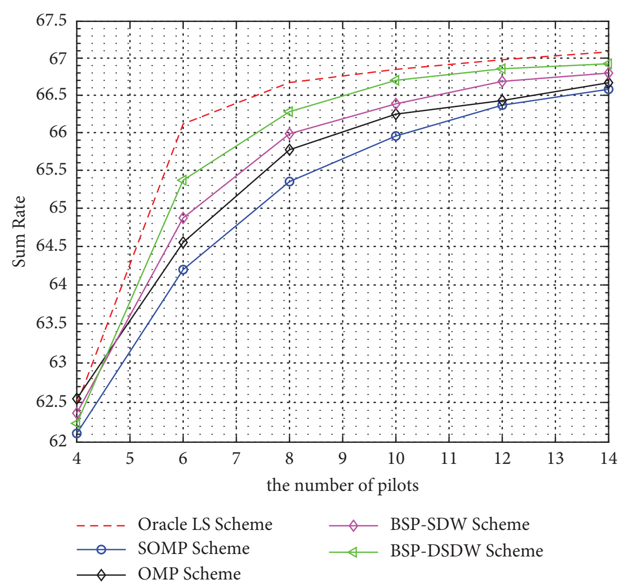

Figure 7: Sum rate of pilot length algorithms.

The complexities of the OMP and SOMP algorithms are also analyzed in the same way. Both channel estimations are iterated based on the LS principle, and the complexity is $O(LNN_{RF}QK\lambda) + O(LN_{RF}QL^3\lambda^3)$. Compared with the two algorithms, the dynamic window λ of this paper is smaller, which is one N order less than that of N. Therefore, the complexity is reduced.

5. Simulation Results and Analysis

This section considers simulation results for massive MIMO systems in broadband systems and compares and analyzes various algorithms. Parameter settings: the number of antennas is 256, number of users is 8, number of radio frequency chains $N_{RF} = 8$, center carrier frequency $f_c =$ 30GHz, bandwidth $B = 4$ GHz, and the number of subcarriers is 512. The specific channel parameters are set as the number of paths which is 3, the spatial direction $\varphi_l \in \mathcal{U}(-\pi/2, \pi/2)$, and the path time delay $\tau_l = 20$ns. The normalized mean square error is used as a measure of channel estimation.

Figure 4 illustrates the normalized mean square error (NMSE) of the corresponding algorithms under different SNRs. In addition, the Oracle LS scheme is employed as a reference, where the channel support set on all subcarriers is known. Due to the consideration in SOMP [26] of different sparse signals sharing the same support set and the influence of wave number splitting in mmWave massive

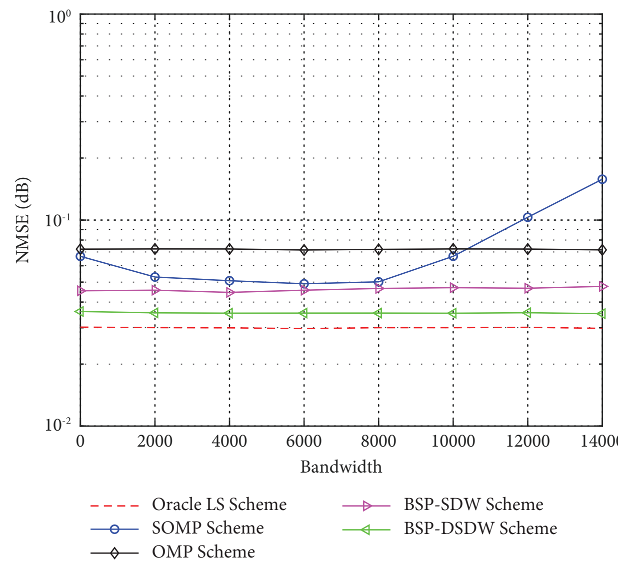

FIGURE 8: NMSE performance of each algorithm under different bandwidths.

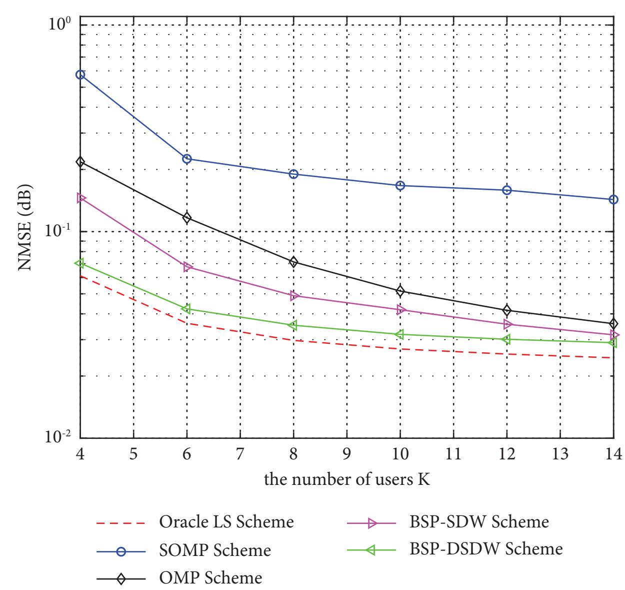

FIGURE 9: NMSE performance of each algorithm under different user numbers.

MIMO systems, its performance is not ideal. In contrast, the OMP [27] algorithm considers unique sparse parts in its sparse model. During the iteration process, signal recovery is performed using the residual of a single sparse signal, leading to improved accuracy. The BSP-SDW and BSP-DSDW algorithms capture the physical channel direction of subcarriers, obtaining support sets for different sparse signals, thereby effectively addressing the impact of wave number splitting. Furthermore, BSP-DSDW enhances algorithm performance by incorporating a moving window. In terms of channel estimation accuracy, BSP-DSDW gradually approaches the Oracle LS scheme. The dynamic window method effectively expands the support set using power calculation. However, as compressive sensing methods may approximate some lower-energy elements to zero, while it cannot fully approach the Oracle LS scheme, its performance gradually stabilizes with increasing SNR.

To comprehensively evaluate the performance of the proposed channel estimation algorithms, in Figure 5, we compare the performance of the algorithms under different SNR conditions using the sum rate as a metric. This metric is crucial for meeting users' demands for high-speed and high-quality communication. From the graph, we observe an overall increasing trend in the sum rate with the increase in SNR. It is noteworthy that the sum rate of the BSP-DSDW method gradually approaches that of the Oracle LS method and outperforms BSP-SDW, SOMP, and OMP algorithms. The BSP-DSDW algorithm may achieve sum rates close to the Oracle LS algorithm at lower SNR levels because it focuses on subcarriers with high signal power and can better handle interference between noise and signal during the channel estimation process, thereby improving the sum rate.

Figure 6 details the relationship between pilot length and NMSE for different algorithms when the SNR is set to 20 dB. Meanwhile, Figure 7 shows the trend of sum rate changes under different pilot lengths. As the pilot length increases, the NMSE of all algorithms correspondingly decreases, indicating an improvement in estimation accuracy. The sum rate also shows a gradual upward trend, which can be explained by the more accurate acquisition of channel state information, allowing for a better resource allocation and signal modulation, ultimately enhancing the system's sum rate. Among the algorithms, BSP-DSDW demonstrates significant advantages in both NMSE and sum rate performance, with results closely matching those of the Oracle LS algorithm. This indicates that BSP-DSDW can achieve high performance with lower pilot overhead while meeting the same accuracy requirements.

Figure 8 shows the impact of bandwidth on the NMSE estimation characteristics of different algorithms. The SNR is set to 15 dB, and the number of pilot groups is set to 10. It can be seen that when the bandwidth is small, such as 8 GHz, SOMP can also achieve good results because, at low frequencies, the wave number splitting effect has a weak impact on channel estimation. Thus, the same common sparse signal estimation method can also achieve satisfactory performance. However, as the bandwidth increases, the wave number splitting effect becomes significant, and the support sets of different subcarriers for broadband beamspace vary greatly, resulting in a decrease in estimation performance. BSP-DSDW, by dynamically adjusting the detection window and effectively expanding the support set, can better cope with the wave number splitting effect. Even under high bandwidth conditions, BSP-DSDW can accurately capture the physical channel directions of different subcarriers, maintaining high channel estimation accuracy. Therefore, the BSP-DSDW algorithm demonstrates superior performance across various bandwidths.

The number of antennas set in this study is fixed. Figure 9 shows the NMSE performance comparison of each algorithm for different numbers of users, with the SNR set to 10 dB. As the number of users increases, it can be observed that the performance of the BSP-DSDW algorithm significantly decreases but then gradually stabilizes. The BSP-DSDW algorithm enhances signal coverage by dynamically adjusting the detection window and effectively expanding the support set. When the number of users increases, although the number of pilots also increases, potentially leading to increased estimation errors of the common support set, the BSP-DSDW algorithm is better able to handle this interference. By focusing on subcarriers with high signal power, it maintains a high level of channel estimation accuracy. This demonstrates that the proposed BSP-DSDW algorithm has a high stability when facing an increasing number of users and can effectively maintain performance in multiuser environments.

6. Conclusion

In this paper, we have conducted research on channel estimation for mmWave massive MIMO systems, with a particular focus on addressing the challenges posed by the wave number splitting effects in such systems. It is important to note that the assumption that common sparse signals share the same support set no longer holds true in this context; instead, the sparse support for different subcarriers varies. Consequently, this paper employs a method rooted in physical direction detection, primarily aimed at estimating the physical direction. This approach establishes a one-to-one correspondence between the index of elements in different directions and their respective physical directions, effectively mitigating the challenges introduced by beam-splitting effects. After framing the channel estimation problem as a beam direction estimation issue, we propose a channel estimation scheme. Leveraging the physical direction obtained via the BSP algorithm as the index set, in combination with a dynamic window expansion method, we obtain the support set with maximum power. This approach significantly enhances the accuracy of support set acquisition. Through simulation and algorithm performance comparison analysis, it is observed that the BSP-DSDW method is better than other methods in terms of NMSE and sum rate and is very close to the performance of the Oracle LS method [28].

Data Availability

The data used to support the findings of this study are available from the corresponding author upon request.

Conflicts of Interest

The authors declare that there are no conflicts of interest regarding the publication of this paper.

Acknowledgments

This work was supported by the National Natural Science Foundation of China (Grant no. 62371428) and Fundamental Research Funds for the Central Universities (CUC23GG13).

References

[1] M. Borhani-Kakhki, A. Dadgarpour, M. A. Antoniades, A. R. Sebak, and T. A. Denidni, "Magnetoelectric dipole antennas loaded with meta-lens for 5G MIMO pattern diversity applications," *IEEE Transactions on Antennas and Propagation*, vol. 70, no. 8, pp. 7112–7117, 2022.

[2] R. Nissel, "Correctly modeling TX and RX chain in (distributed) massive MIMO new fundamental insights on coherency," *IEEE Communications Letters*, vol. 26, no. 10, pp. 2465–2469, 2022.

[3] Q. Wu, J. Jing, X. W. Zhu, and C. Yu, "Digital predistortion for concurrent dual-band millimeter wave analog multibeam transmitters," *IEEE Transactions on Circuits and Systems II: Express Briefs*, vol. 69, no. 3, pp. 1747–1751, 2022.

[4] F. Liu, P. Zhao, and Z. Wang, "EKF-based beam tracking for mmWave MIMO systems," *IEEE Communications Letters*, vol. 23, no. 12, pp. 2390–2393, 2019.
[5] T. Lin and Y. Zhu, "Beamforming design for large-scale antenna arrays using deep learning," *IEEE Wireless Communications Letters*, vol. 9, no. 1, pp. 103–107, 2020.
[6] F. Lei, Z. Fang, Y. Xu et al.,, "An improved compression sampling matching tracking algorithm," *Optical Communication Research*, vol. 228, no. 6, pp. 72–76, 2021.
[7] Y. Xiong, "A generalized VAMP-based channel estimator for uplink quantized massive MIMO systems," *IEEE Transactions on Vehicular Technology*, vol. 69, no. 6, pp. 6838–6842, 2020.
[8] F. Bellili, F. Sohrabi, and W. Yu, "Generalized approximate message passing for massive MIMO mmWave channel estimation with laplacian prior," *IEEE Transactions on Communications*, vol. 67, no. 5, pp. 3205–3219, 2019.
[9] X. Wu, S. Ma, and X. Yang, "Tensor-based low-complexity channel estimation for mmWave massive MIMO-OTFS systems," *Journal of Communications and Information Networks*, vol. 5, no. 3, pp. 324–334, 2020.
[10] N. Chen, H. Lin, Y. Zhao, L. Huang, X. Du, and M. Guizani, "Low complexity closed loop strategy for mmWave communication in industrial intelligent systems," *International Journal of Intelligent Systems*, vol. 37, no. 12, pp. 10813–10844, 2022.
[11] P. Liu and T. Jiang, "Channel estimation performance analysis of massive MIMO IoT systems with ricean fading," *IEEE Internet of Things Journal*, vol. 8, no. 7, pp. 6114–6126, 2021.
[12] S. G. Yoon and S. J. Lee, "Improved hierarchical codebook-based channel estimation for mmWave massive MIMO systems," *IEEE Wireless Communications Letters*, vol. 11, no. 10, pp. 2095–2099, 2022.
[13] A. M. Elbir and S. Chatzinotas, "BSA-OMP: beam-split-aware orthogonal matching pursuit for THz channel estimation," *IEEE Wireless Communications Letters*, vol. 12, no. 4, pp. 738–742, 2023.
[14] X. Su, R. He, B. Ai, Y. Niu, and G. Wang, "Channel estimation for RIS assisted THz systems with beam split," *IEEE Communications Letters*, vol. 28, no. 3, pp. 637–641, 2024.
[15] K. Xu, Z. Shen, Y. Wang, and X. Xia, "Location-aided mMIMO channel tracking and hybrid beamforming for high-speed railway communications: an angle-domain approach," *IEEE Systems Journal*, vol. 14, no. 1, pp. 93–104, 2020.
[16] E. Balevi, A. Doshi, A. Jalal, A. Dimakis, and J. G. Andrews, "High dimensional channel estimation using deep generative networks," *IEEE Journal on Selected Areas in Communications*, vol. 39, no. 1, pp. 18–30, 2021.
[17] S. Li, Y. Feng, Y. Sun, and Z. Xia, "A low-complexity detector for uplink SCMA by exploiting dynamical superior user removal algorithm," *Electronics*, vol. 11, no. 7, p. 1020, 2022.
[18] A. Mohammed, S. Zhang, H. Li, N. Zhao, and X. Wang, "Capturing the sparsity and tracking the channels for massive MIMO networks," *IEEE Transactions on Vehicular Technology*, vol. 69, no. 1, pp. 685–699, 2020.
[19] A. Meijerink and A. F. Molisch, "On the physical interpretation of the saleh–valenzuela model and the definition of its power delay profiles," *IEEE Transactions on Antennas and Propagation*, vol. 62, no. 9, pp. 4780–4793, 2014.
[20] F. Han, X. Wang, and H. Deng, "A very-low pilot scheme for mmWave hybrid massive MIMO-OFDM systems," *IEEE Wireless Communications Letters*, vol. 10, no. 9, pp. 2061–2064, 2021.
[21] S. Roger, M. Cobos, C. Botella-Mascarell, and G. Fodor, "Fast Channel estimation in the transformed spatial domain for analog millimeter wave systems," *IEEE Transactions on Wireless Communications*, vol. 20, no. 9, pp. 5926–5941, 2021.
[22] Z. Wang, Y. Li, C. Wang, D. Ouyang, and Y. Huang, "A-OMP: an adaptive OMP algorithm for underwater acoustic OFDM channel estimation," *IEEE Wireless Communications Letters*, vol. 10, no. 8, pp. 1761–1765, 2021.
[23] J. Tan and L. Dai, "Wideband Channel estimation for THz massive MIMO," *China Communications*, vol. 18, no. 5, pp. 66–80, 2021.
[24] A. Chatterjee and P. W. T. Yuen, "Sample selection with SOMP for robust basis recovery in sparse coding dictionary learning," *IEEE Letters of the Computer Society*, vol. 2, no. 3, pp. 28–31, 2019.
[25] H. Ghanooni and M. J. Azizipour, "Superposition based downlink channel estimation in large-scale MIMO systems," *Telecommunication Systems*, vol. 83, no. 1, pp. 79–89, 2023.
[26] K. Venugopal, A. Alkhateeb, N. Gonzalez Prelcic, and R. W. Heath, "Channel estimation for hybrid architecture-based wideband millimeter wave systems," *IEEE Journal on Selected Areas in Communications*, vol. 35, no. 9, pp. 1996–2009, 2017.
[27] Z. Gao, C. Hu, L. Dai, and Z. Wang, "Channel estimation for millimeter wave massive MIMO with hybrid precoding over frequency selective fading Channels," *IEEE Communications Letters*, vol. 20, no. 6, pp. 1259–1262, 2016.
[28] J. Sun, M. Jia, Q. Guo, X. Gu, and Y. Gao, "Power distribution based beamspace channel estimation for mmWave massive MIMO system with lens antenna array," *IEEE Transactions on Wireless Communications*, vol. 21, no. 12, pp. 10695–10708, 2022.